Journal of Global Antimicrobial Resistance 37 (2024) 108–121

Contents lists available at ScienceDirect

Journal of Global Antimicrobial Resistance

journal homepage: www.elsevier.com/locate/jgar

Drug efflux and lipid A modification by 4-L-aminoarabinose are key mechanisms of polymyxin B resistance in the sepsis pathogen *Enterobacter bugandensis*

Inmaculada García-Romero[a,e], Mugdha Srivastava[b,c], Julia Monjarás-Feria[a], Samuel O. Korankye[a], Lewis MacDonald[a], Nichollas E. Scott[d], Miguel A. Valvano[a,*]

[a] *Wellcome-Wolfson Institute for Experimental Medicine, Queen's University Belfast, United Kingdom*
[b] *Functional Genomics & Systems Biology Group, Department of Bioinformatics, Biocenter, Am Hubland, University of Wuerzburg, Wuerzburg, Germany*
[c] *Core Unit Systems Medicine, University of Wuerzburg, Wuerzburg, Germany*
[d] *Department of Microbiology and Immunology, University of Melbourne, Melbourne, Australia*
[e] *Centro Andaluz de Biología del Desarrollo, CSIC-Universidad Pablo de Olavide, Sevilla, Spain*

ARTICLE INFO

Article history:
Received 16 December 2023
Revised 27 February 2024
Accepted 14 March 2024
Available online 27 March 2024

Editor: S. Stefani

Keywords:
Intrinsic antibiotic resistance
Outer membrane permeability
Cationic antimicrobial peptides
Enterobacter cloacae complex
Neonatal sepsis
KexD

ABSTRACT

Objectives: A concern with the ESKAPE pathogen, *Enterobacter bugandensis*, and other species of the *Enterobacter cloacae* complex, is the frequent appearance of multidrug resistance against last-resort antibiotics, such as polymyxins.
Methods: Here, we investigated the responses to polymyxin B (PMB) in two PMB-resistant *E. bugandensis* clinical isolates by global transcriptomics and deletion mutagenesis.
Results: In both isolates, the genes of the CrrAB-regulated operon, including *crrC* and *kexD*, displayed the highest levels of upregulation in response to PMB. Δ*crrC* and Δ*kexD* mutants became highly susceptible to PMB and lost the heteroresistant phenotype. Conversely, heterologous expression of CrrC and KexD proteins increased PMB resistance in a sensitive *Enterobacter ludwigii* clinical isolate and in the *Escherichia coli* K12 strain, W3110. The efflux pump, AcrABTolC, and the two component regulators, PhoPQ and CrrAB, also contributed to PMB resistance and heteroresistance. Additionally, the lipid A modification with 4-L-aminoarabinose (L-Ara4N), mediated by the *arnBCADTEF* operon, was critical to determine PMB resistance. Biochemical experiments, supported by mass spectrometry and structural modelling, indicated that CrrC is an inner membrane protein that interacts with the membrane domain of the KexD pump. Similar interactions were modeled for AcrB and AcrD efflux pumps.
Conclusion: Our results support a model where drug efflux potentiated by CrrC interaction with membrane domains of major efflux pumps combined with resistance to PMB entry by the L-Ara4N lipid A modification, under the control of PhoPQ and CrrAB, confers the bacterium high-level resistance and heteroresistance to PMB.

1. Introduction

Most Gram-negative bacterial species from the *Enterobacter* genus [1,2] are commonly found in the human gut microbiota and as opportunistic pathogens causing bacteraemia, intra-abdominal infections, and infections in multiple sites [1]. Because of the emergence of multidrug resistant isolates, *Enterobacter* species are included in the ESKAPE list of global threat pathogens requiring treatment with last-resort antibiotics, such as polymyxins [3]. One of these species, *Enterobacter bugandensis*, is predominantly associated with neonatal sepsis [4–6].

Polymyxin B (PMB) and E (colistin) are cationic antimicrobial peptides active against Gram-negative bacteria; they bind the bacterial outer membrane by interacting with negative charges in the lipid A moiety of the lipopolysaccharide (LPS) and displacing Mg^{2+} ions that crosslink LPS molecules at the outer membrane surface, thereby promoting their own uptake [7]. Recent evidence suggests polymyxins also target nascent LPS molecules in the inner membrane [8]. Unfortunately, polymyxin resistant *Enterobacter* strains

* Corresponding author at: The Wellcome-Wolfson Institute for Experimental Medicine, Queen's University Belfast, 97 Lisburn Rd. Belfast, BT9 7BL, United Kingdom.
E-mail address: m.valvano@qub.ac.uk (M.A. Valvano).

https://doi.org/10.1016/j.jgar.2024.03.012

have appeared [9,10], including those with heteroresistant phenotypes [11–14].

Bacteria resist polymyxins through chemical modifications of lipid A that reduce their overall negative charge; these generally involve covalent addition of 4-amino-4-deoxy-L-arabinose (L-Ara4N) or phosphoethanolamine (PEtN) onto the free phosphates of lipid A, and the removal of free phosphates [15]. Bacteria can also modify the number, length, and hydroxylation of lipid A acyl chains, which augments lipid A membrane packing, further reducing the outer membrane permeability to cationic antimicrobial peptides [15,16]. Like in other bacteria, the *Enterobacter* PhoPQ two-component system (TCS) regulates the transcription of the LPS-modifying genes [12,17]. An *Enterobacter* small transmembrane protein, Ecr, also enhances the transcription of the L-Ara4N biosynthesis gene cluster via PhoPQ [18], while MgrB negatively regulates PhoPQ; several mutations have been described in the *Enterobacter mgrB* gene that lead to colistin resistance [13,19]. Plasmids carrying *mcr* genes, which encode lipid A PEtN transferases and drive the spread of PMB/colistin resistance by horizontal gene transmission [20], have also been documented in *Enterobacter* clinical isolates [2,13].

The AcrAB-TolC is a well characterized efflux pump consisting of an integral membrane protein, AcrB, a periplasmic anchor, AcrA, and the outer-membrane channel TolC [21]. This pump contributes to PMB/colistin heteroresistance in *Enterobacter asburiae* and *Enterobacter cloacae* [22]. The CrrAB, CrrC and KexD proteins were recently identified in several *Enterobacter* species, including *E. bugandensis*, and implicated in colistin resistance [23]. KexD, initially described in *Klebsiella pneumoniae* [24,25], is an AcrB ortholog encoded in the same operon with CrrC, a predicted small transmembrane protein. Unlike AcrB, KexD is not encoded together with a periplasmic lipoprotein anchor (such as an AcrA ortholog) [24,25]. The TCS CrrAB regulates the expression of the *crrC* and *kexD* genes [24,26]. The CrrC protein is predicted to activate *pmrAB* expression in *K. pneumoniae*, which in turn activates lipid A modification mechanisms inducing high-level PMB resistance [26,27]; however, the CrrC mechanism of action is unknown.

In this study, we investigated PMB resistance and heteroresistance in two highly resistant *E. bugandensis* clinical isolates by global transcriptomics and gene deletion approaches. *Enterobacter bugandensis* is one of the *Enterobacter* species that exhibits high intrinsic resistance to polymyxins [10,13,23]. We show that *crrC* and *kexD* were among the highest upregulated genes in response to PMB. Biochemical experiments, mass spectrometry, and structural modelling demonstrated that CrrC is a membrane protein that interacts with the N-terminal membrane domain of KexD and similar domains of AcrB and AcrD proteins. Our results provide a model whereby drug efflux potentiated by CrrC interactions with major efflux pumps, combined lipid A modifications preventing PMB entry, under the control of PhoPQ and CrrAB, confers *E. bugandensis* high-level resistance and heteroresistance to PMB.

2. Materials and methods

2.1. Bacterial strains and culture conditions

Escherichia coli K12, *E. bugandensis*, and *Enterobacter ludwigii* strains were grown in lysogeny broth (LB) or cation-adjusted Mueller-Hinton (CAMH) at 37°C. When required, media were supplemented with gentamicin or kanamycin at final concentrations of 25 and 20 µg/mL, respectively, or PMB to reach final concentrations ranging from 1–2048 µg/mL. Deletion mutants in *Enterobacter* species were constructed using the λ-red recombinase system, as previously reported [28] (Supplementary Materials). Strains and plasmids used are listed in Supplementary Table S1.

2.2. Genome sequencing, annotation, and in silico taxonomy

E. bugandensis E105227 and E104107 genomes were sequenced by MicrobesNG (Birmingham, UK) and annotated as described in Supplementary Materials. The complete sequences were deposited in the National Centre for Biotechnology Information (NCBI) under BioProject numbers PRJNA901438 and PRJNA901437, respectively, with GenBank accession numbers CP110985 (chromosome), CP110986 (plasmid) and CP110987 (plasmid) for E105227 and CP110983 (chromosome) and CP110984 (plasmid) for E104107. The draft genome sequence of *E. ludwigii* E2618 was deposited in NCBI under BioProject number PRJNA950081 with GenBank accession number JARRIP000000000. The species assignment for E105227 and E104107 was determined by calculating their overall genome relatedness index based on whole-genome average nucleotide identity measurements using FastANI [29], and by digital DNA:DNA hybridization using the Type Strain Genome Server (TYGS) with default parameters [30] (Supplementary Materials).

2.3. RNA extraction, sequencing, and data analyses

E105227 and E104107 were grown until exponential phase in 10 mL of LB with and without PMB (64 µg/mL for E104017 and 256 µg/mL for E105227). RNA was extracted from bacterial pellets using Direct-zol RNA Miniprep Plus (Zymo Research), following the manufacturer's instructions and RNA integrity and purity were checked in a 1% agarose gel. RNA extractions were performed in triplicate for each condition/strain. RNA samples were processed for RNA-seq by the Core Unit Systemmedizin (SysMed) in the Institut für Molekulare Infektionsbiologie (IMIB) (Wurzburg, Germany). After passing quality controls, DNA libraries were prepared from 100 ng of total RNA using the TruSeq Stranded Total RNA library preparation kit combined with Illumina Ribo-Zero Plus for rRNA depletion. Sequencing of pooled libraries, spiked with 1% PhiX control library, was performed at 12 million reads/sample in single-end mode with 75 nt read length on the NextSeq 500 platform (Illumina) using the High output sequencing kit. Demultiplexed FASTQ files were generated with bcl2fastq2 v2.20.0.422 (Illumina). Illumina reads were quality and adapter trimmed with Cutadapt56 v.2.5 [31] using a cut-off Phred score of 20 in NextSeq mode, and reads with no remaining bases were discarded (command line parameters: –nextseq-trim = 20 -m 1 -a AGATCGGAAGAGCACACGTCTGAACTCCAGTCAC). READemption57 v.0.4.5 [32] to align all reads to the respective reference sequences using segemehl58 v.0.2.0 [33] with an accuracy cutoff of 95% (-α 95). We used READemption gene quanti to quantify aligned reads, overlapping genomic features by at least 10 nt (-o 10). For this, we provided annotations (CDS, ncRNA, rRNA, tmRNA, and tRNA) from the assemblies of E105227 and 132E104107 in GFF format [34]. Differential gene expression analysis was performed by DESeq2 [35] version 1.24.0. with genes considered significantly enriched at an adjusted P value (padj) <0.05 and $\log_2$FcCutoff ≥ 1.0. The RNA-Seq raw data have been deposited in NCBI's Gene Expression Omnibus (GEO) and are accessible through GEO accession number GSE218614. Orthologs protein between E105227 and E104107 were obtained using the script getRBH.pl [36] and selecting the program diamond and the very-sensitive option. Then, common genes within upregulated or downregulated sets were calculated using Venny 2.1 [37].

2.4. Biological enrichment and protein-protein interaction network analysis

Upregulated and downregulated genes in the presence of PMB were analysed by biological enrichment according to the annotated GO terms using the Fisher's exact test and the R package

TopGO version 2.42.0 applying the weight01 algorithm [38] and plotted using the R package ggplot2 [39]. For the network analysis, high-confidence protein-protein interactions (PPIs) and their corresponding amino acid sequences of Gram-negative bacilli of the genera *Enterobacter, Escherichia, Klebsiella, Serratia*, and *Citrobacter* were downloaded from String database version 11.5. These PPIs were used as template for reconstructing an interolog-based interactome [40] of *E. bugandensis* E105227. Inparanoid [41] was used to identify orthologous relationships. Topological analysis of the interactome was performed with the Network Analyser plugin, version 2.7, of Cytoscape version 2.8.173 [42].

2.5. Polymyxin B susceptibility testing and population analysis profile

Minimum inhibitory concentration values were determined by broth microdilution performed in triplicate for PMB concentrations between 1–2048 µg/mL, as described previously [43], except that LB was used in keeping with the conditions employed for mRNA seq. Dilutions were performed in honeycomb 100-well plates (Oy Growth Curves Ab, Ltd., Finland), which were incubated in a Bio-Screen C (Dynex ČR, Buštěhrad, Czech Republic) at 37°C for 24 h with shaking with automatic readings of optical density at 600 nm (OD600) taken every 30 min. The population analysis profile (PAP) was performed as described previously [43]. Isolates were defined as heteroresistant when the antibiotic concentration exhibiting the highest inhibitory effects was 8-fold higher than the highest non-inhibitory concentration [43,44]. To compare across the different strains and mutants, PAP data were represented by calculating the area under the curve (AUC) from 0–24 h and indicating the percent AUC at each PMB concentration, relative to the AUC value without PMB. The AUC was calculated using Graph Pad Prism 9. E-test was performed according to the manufacturer's instructions (bioMérieux) in bacteria grown overnight in LB or CAMH, refreshed to exponential phase, then resuspended in 0.85% NaCl, and adjusted to OD_{600} 0.1.

2.6. Complementation and heterologous expression of candidate genes

For genetic complementation of deletion mutants, the required genes were amplified by PCR (oligonucleotides are listed in Supplementary Table S2) and cloned by Gibson assembly [45] into the plasmid pDA17Km, which was previously cut with *Xba*I. Once cloned, the genes were under the control of the constitutive *dhfr* gene promoter and the expressed proteins were C-terminally fused to a FLAG epitope tag. Plasmids were introduced into the mutants by electroporation; empty pDA17Km was introduced in all the strains as a control.

2.7. Pull-downs and co-immunoprecipitation

For pull-downs, a 200-mL LB culture of Δ*crrC*/pDA17Km_*crrC* (expressing $CrrC_{FLAG}$) was grown at 37°C, with shaking for 5 h. In parallel, 200-mL LB cultures of *E. coli* BL21 expressing either *KexD6xHis* or *AcrB6xHis* were grown with 0.5 mM IPTG at 30°C with shaking for 4 h. After centrifugation, cell pellets were resuspended in Tris 20 mM, NaCl 250 mM, pH 7.4, with a dissolved protease inhibitor tablet (Roche), and lysed using a cell disruptor (Constant Systems). Lysates were incubated with 1% n-dodecyl-β-D-maltoside (DDM) for 2 h and then cleared by centrifugation at 11,000 rpm for 30 min. Supernatants were combined with 1 mL of Ni-NTA resin, incubated overnight with shaking, and the next day, columns were washed using 50 mM and 80 mM imidazole and proteins eluted using 500 mM imidazole. Proteins were separated by polyacrylamide gel electrophoresis and examined by western blot with anti-FLAG M2 (Sigma) or anti-His (Sigma) antibodies, reacted with IRDye 800CW Goat anti-Mouse IgG (H + L), or IRDye 680CW Goat anti-Mouse IgG (H + L) (LI-COR), and fluorescence examined using a LI-COR Odyssey infrared imaging system. For co-immunoprecipitations, cell cultures were processed as indicated above, except that bacterial pellets were resuspended with HEPES 20 mM, NaCl 250 mM pH 7.4, and protease inhibitor (Roche) before lysis. Cell lysates were incubated with 1% DDM for 2 h and, after clearing by centrifugation, supernatants were treated with disuccinimidyl suberate at a final concentration of 1 mM. After 1-h incubation at room temperature, the crosslinking reaction was stopped by adding 20 mM Tris pH 7.5 for 15 min and samples were mixed with 100 µL of anti-FLAG M2 Affinity Gel beads (Sigma) and incubated overnight at 4°C with shaking. *CrrCFLAG*-coupled beads were centrifuged at 4000 rpm for 15 min and washed twice with HEPES 20 mM, 0.1% DDM, NaCl 250 mM pH 7.4. The beads were resuspended in 100 µL of SDS-PAGE sample buffer and boiled for 5 min. Protein samples were resolved by SDS-PAGE and analysed by immunoblotting using anti-FLAG antibody (Sigma). Bands containing CrrC-FLAG and the co-isolated proteins were excised for protein identification by mass spectrometry.

2.8. Mass spectrometry and protein identification

Immunoprecipitated protein bands of interest were digested with trypsin [46] and subjected to LC-MS Dionex Ultimate 3000 UPLC (Thermo Fisher Scientific) coupled to an Orbitrap Fusion™ Lumos™ Tribrid™ Mass Spectrometer equipped with a FAIMS Pro interface (Thermo Fisher Scientific) (Supplementary Methods). The *E. bugandensis* CrrC interaction partners were identified using MaxQuant (v1.6.17.0) [47]. The outputs were processed within Perseus (v1.4.0.6) [48] to remove reverse matches and contaminants. The resulting mass spectrometry (MS) data and search results were deposited into the PRIDE ProteomeXchange Consortium repository under the identifier PXD042287.

2.9. Membrane protein isolation and immunoblotting

Cultures of Δ*kexD*/pKDA17Km, Δ*crrC*/pIGR02, Δ*kexD*/pIGR05, and Δ*crrCkexD*/pIGR05 were incubated until exponential phase and processed for lysis as described above. Total membranes were isolated by centrifugation at 42,220 xg at 4°C for 1 h and resuspended in 50 µL of 50 mM Tris-HCl pH 8 prior to SDS-PAGE and western blotting, as described above.

2.10. Lipid A mass spectrometry

Matrix-assisted laser desorption/ionization-time of flight (MALDI-TOF) MS was used to characterize the lipid A modifications present in the LPS of strains challenged with PMB. The lipid A extraction and analysis was performed as described in [49] (Supplementary Methods) using a Bruker Autoflex MALDI-TOF mass spectrometer in reflectron mode, negative-ion polarity mode. Data acquisition and analysis were performed with the Bruker zed with the Bruker Flex Analysis software.

2.11. *Galleria mellonella* infection

The bacterial inoculum was prepared by refreshing overnight cultures in LB to mid-log phase (OD_{600} 0.6) and adjusting to OD_{600} 0.001 ($\sim 10^5$ CFU/ml) in phosphate-buffered saline (PBS). *Galleria mellonella* larvae (UK Waxworms Ltd.) were inoculated using 10 µL of the respective bacterial suspension by injection into the rear proleg of each larva. Ten larvae were infected for each isolate and the infections were repeated three times. Larvae were also injected with the same volume of PBS as a control. Survival ratio was measured daily over five days.

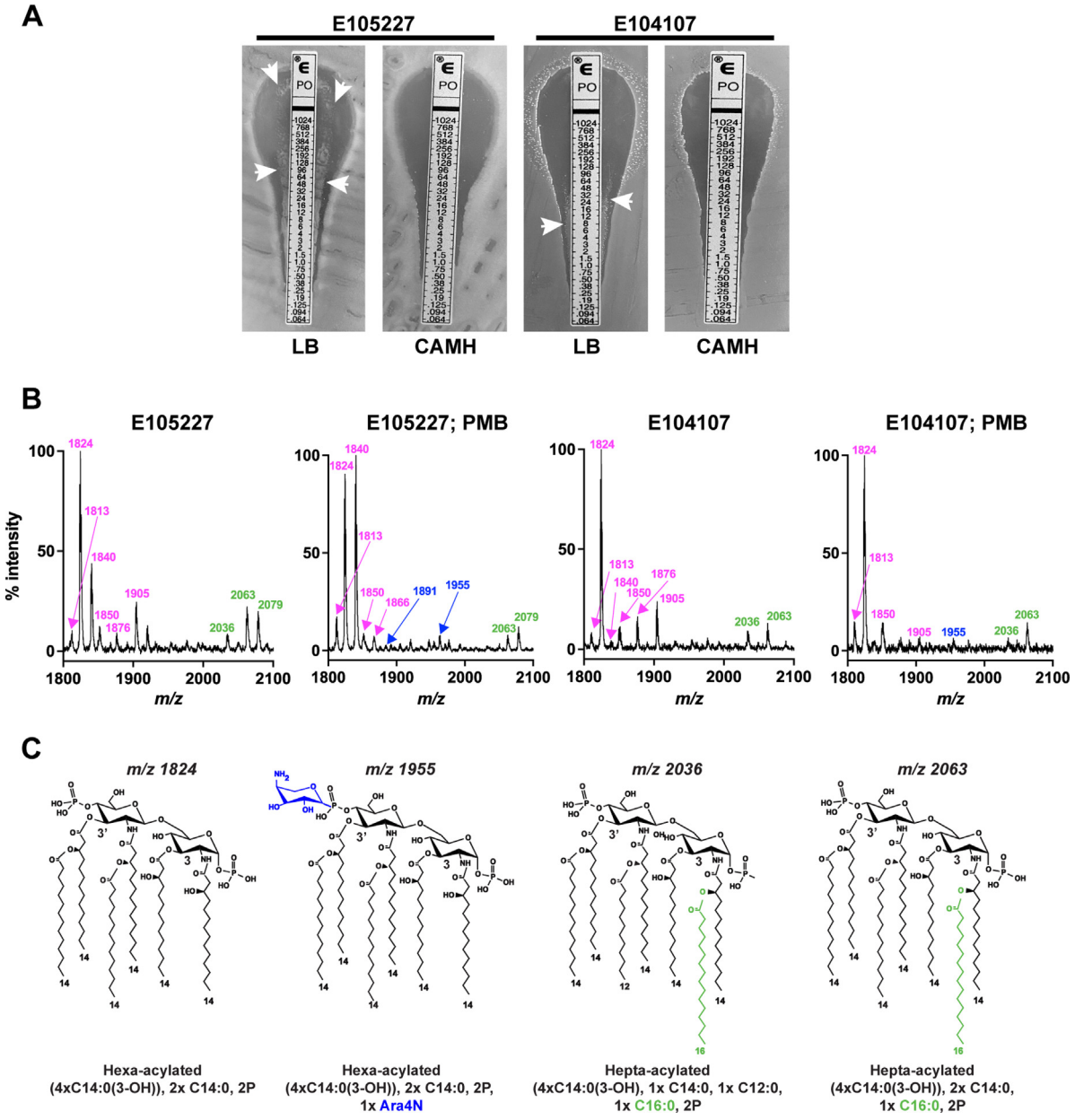

Fig. 1. E-test and MALDI-TOF MS lipid A spectra of E105227 and E104107 strains. (A) E-test was performed in LB and CAMH media. The heteroresistant phenotype is denoted by the colonies growing within the inhibition area in LB (arrows). (B) lipid A analysis by negative ion reflectron MALDI-TOF mass spectrometry. Lipid A was extracted from bacterial cultures grown to log phase in LB with or without PMB challenge. Assigned *m/z* ion peaks in blue represent lipid A forms containing L-Ara4N; ion peaks in green represent lipid A forms containing palmitate (C16:0). The predicted composition of all detected ion peaks is listed in Supplementary Table S2. (C) Proposed lipid A structures of the main *m/z* ion peaks identified in panel B.

3. Results

3.1. Characterization of the E105227 and E104107 isolates

Strains E105227 and E104107 were reported in a previous study of 95 *E. cloacae* complex clinical isolates representing multiple species [10]. Both strains belonged to the same genogroup and exhibited intrinsic resistance to polymyxins based on broth microdilution in CAMH (MIC for PMB was >1024 µg/mL and 512 µg/mL for E105227 and E104107, respectively) [10]. However, the presence of skipped wells in the microdilution assays suggested that both isolates displayed PMB heteroresistance. These observations were confirmed using E-test (Fig. 1A), which demonstrated bacterial colonies within the inhibition halos, especially upon culturing in LB (Fig. 1A). The different MIC values by microdilution and E-test were expected because the latter assay is unreliable to determine PMB resistance levels [50–52]. We established the complete genome sequence (Supplementary Table S3) of both strains and assigned them as *E. bugandensis* by *in silico* taxonomy approaches; the two strains were highly related among themselves and with the *E. bugandensis* type strain EB-247 (Supplementary Fig. S1). Because resistance to polymyxins primarily depends on LPS modifications, we inferred the lipid A structures of both isolates by comparing matrix-assisted laser desorption/ionization-time of flight (MALDI-TOF) mass spectrometry (MS) profiles from untreated and PMB-treated (10 µg/mL) pairs. The lipid A MS spectrum from bacteria grown without PMB revealed a prominent ion peak at *m/z* 1824 (Fig. 1B and C), corresponding to hexa-acylated lipid A. Modified forms of these peaks, such as the addition of a hydroxyl group (*m/z* +16) to 1824 (*m/z* 1840) and a palmitate

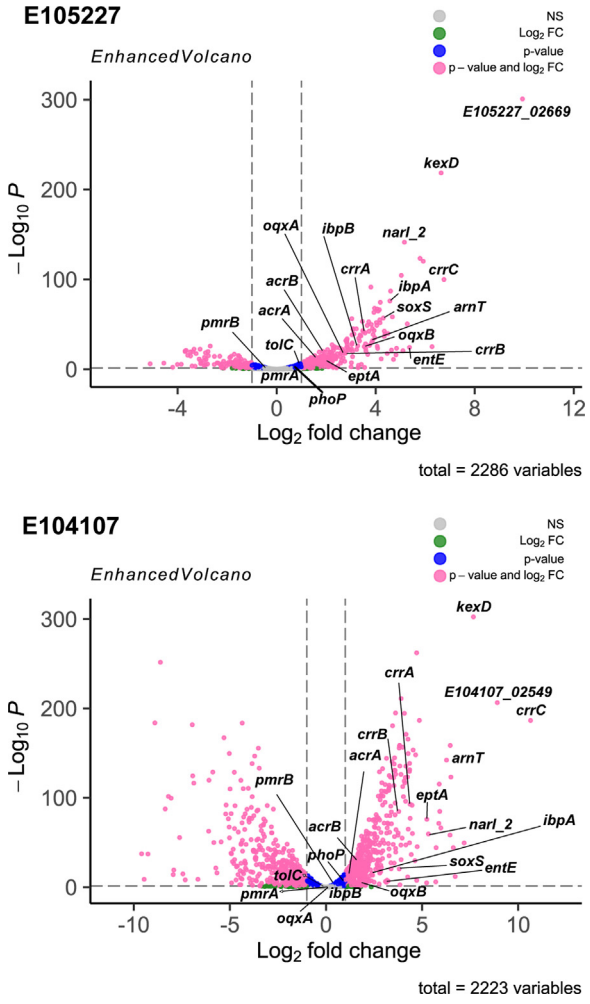

Fig. 2. Volcano plots showing up (>1 Log_2 FC) and down (<1 Log_2 FC) regulated genes in the presence of PMB when compared with control non-treated condition using in both cases a *padj* = 0.05. (A) Shows the E105227 data. The labelled genes were deleted and (B) Shows the E104107 data. In both strains, the highest upregulated genes are *crrC*, *kexD*, and the homologs to the glycosyltransferase H239_3059 (*K. pneumoniae*), which are E105227_02669 and E104107_02549 in E105227 and E104107, respectively. Only genes with an annotated gene name are showed, except for E105227_02669 and E104107_02549.

group (*m/z* +250) to 1813 (*m/z* 2063), were also present (Fig. 1C, Supplementary Table S4). The spectrum of the PMB-challenged isolates displayed a characteristic small peak (*m/z* 1955), which either was absent in the unchallenged isolates or had increased intensity in response to PMB (Fig. 1B, C). This peak denotes the addition of L-Ara4N (*m/z* +131) to the *m/z* 1824 hexa-acyl species. We concluded that when grown with PMB, the lipid A of E105227 and E104107 becomes less electronegative and more acylated (by addition of L-Ara4N and palmitate, respectively), consistent with augmented PMB resistance.

3.2. Transcriptomic analysis identifies global adaptive changes in E. bugandensis isolates upon polymyxin B challenge

We characterized the bacterial response to PMB by performing a comparative global transcriptomic analysis of both E105227 and E104107 grown to exponential phase with and without PMB. Of the 5274 and 4690 total genes in E105227 and E104107, respectively, 632 and 1052 were upregulated (>1 Log_2 FC) and 507 and 1139 (<1 Log_2 FC) were downregulated in response to PMB (Fig. 2) [34]. Among the upregulated genes, 342 are shared between the two strains, while 322 are common within the downregulated genes. Biological enrichment analysis of the transcripts identified global upregulation of genes involved in protein translation, biosynthesis of LPS and polysaccharides, antibiotic responses, iron homeostasis, protein folding, and nitrate assimilation (Supplementary Fig. S2, Supplementary Table S5). Downregulated genes were functionally enriched in cell motility, chemotaxis, TCA cycle, fatty acid β-oxidation, and response to amino acids (Supplementary Fig. S2, Supplementary Table S5). These results indicated that PMB in both strains induces similar metabolic changes related, directly or indirectly, to the effect of this peptide on the disorganization of the outer membrane, as well as cytoplasmic membrane functions associated with active transport and respiratory electron transfer. Given the similarity between the two strains in the transcriptional response to PMB, we performed all subsequent studies on E105227. Because the biological enrichment has the limitation that genes missing GO terms are ignored, we also constructed a protein network analysis of the E105227 proteome (Supplementary Fig. S3). The network analysis was based on combining RNAseq data and the protein-protein interactions (PPIs) data available for genera related to *Enterobacter* (Supplementary Fig. S3) [34]. This analysis revealed that the functional category containing more proteins was siderophore biosynthesis; most of these proteins corresponded to the upregulated genes detected by RNAseq. Similarly, efflux system, oxidative phosphorylation, NAD-dependent oxidoreductase, nitrogen metabolism, and bacterial secretion system networks included proteins that were upregulated in response to PMB. In contrast, flagellar biosynthesis, biofilm formation, quorum sensing, and ABC transporter networks contained only downregulated proteins. One additional network described as cationic antimicrobial peptide resistance also contained downregulated genes that corresponded to homologues of the *sap* operon described *Salmonella* Typhimurium [53], which in *E. bugandensis* is not upregulated upon PMB treatment. Together, the functional analysis of the transcriptomic responses to PMB reveals that proteins predicted to be involved in membrane homeostasis are upregulated, suggesting they may be required to overcome the effects of PMB on membrane integrity. In contrast, functions required for bacterial cell motility and biofilm formation are downregulated, in agreement with previous observations in other bacteria when exposed to polymyxins and other antimicrobial peptides [54,55].

The metabolic changes observed with PMB treatment prompted us to investigate whether the most upregulated genes in metabolic functions bear a relationship with PMB resistance and heteroresistance. We constructed a series of deletion mutants in the strain E105227, including *wcaJ* (colanic acid capsule synthesis), *soxS* (oxidative stress), *narI* (nitrate respiration), *entE* (siderophore biosynthesis), and *ibpAB* (protein folding stress) genes. Both wild-type and mutant strains were examined by population analysis profiling (PAP) and E-test. No differences were found in any of the mutants in comparison to the wild-type strain (Fig. 3A). We conclude that the individual functions of these genes do not play a direct role in PMB resistance, suggesting that their increased transcriptional activity under PMB treatment is the result of global metabolic adaptions to the antibiotic.

3.3. Polymyxin resistance and heteroresistance in E. bugandensis requires lipopolysaccharide remodeling and the activity of efflux pumps

We next investigated the role of genes involved in remodelling the lipopolysaccharide, such as *arnT* and *eptA*, and the TCS regulator genes *phoPQ* and *pmrAB*, as well as *crrC*, *kexD*, and *02669*, which were among the highest upregulated genes in both E105227 and E104107. The *02669* gene is an ortholog of the *K. pneumoniae* H239_3059 gene. Examination of the 02669 polypeptide with HH-

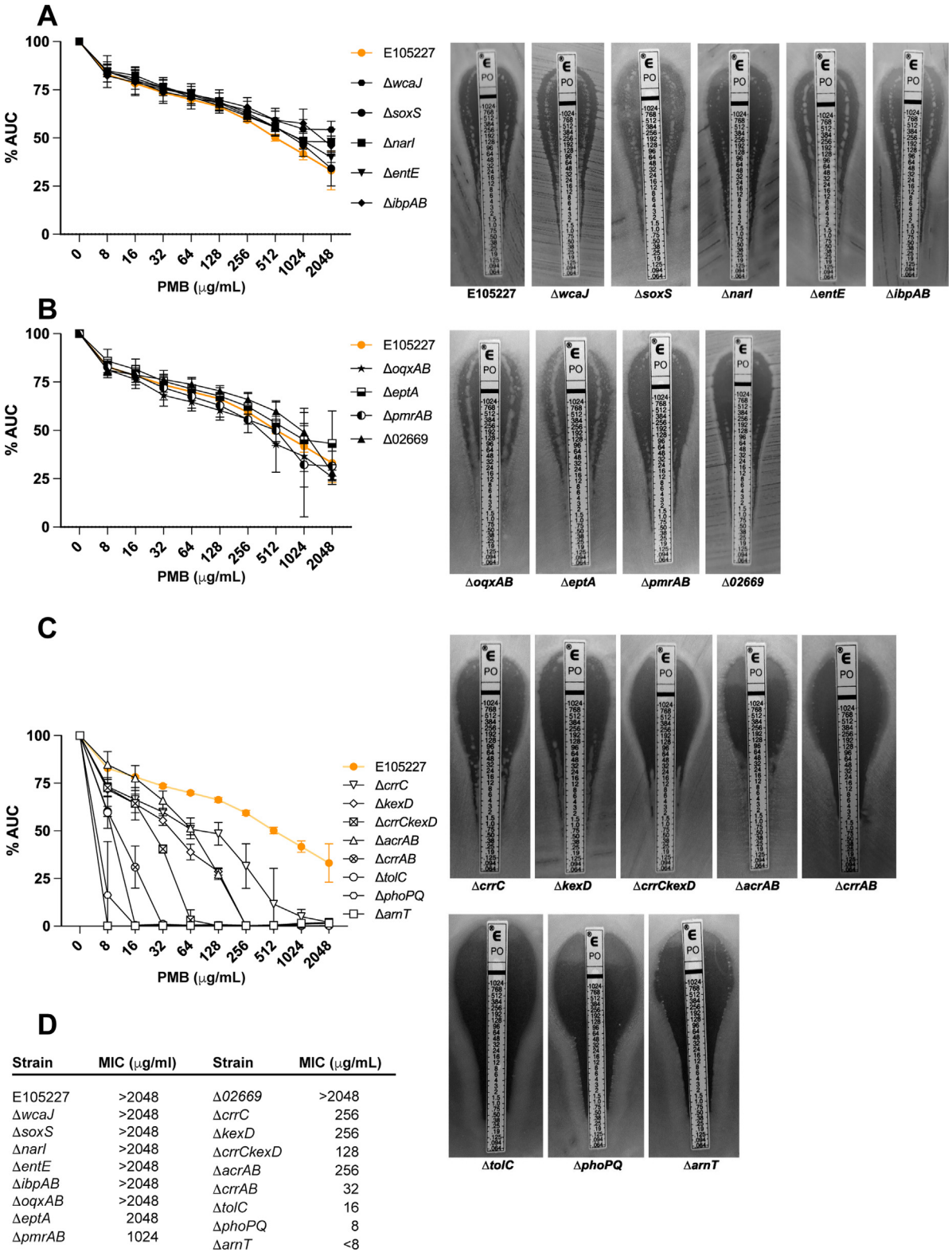

Strain	MIC (μg/ml)	Strain	MIC (μg/mL)
E105227	>2048	Δ02669	>2048
ΔwcaJ	>2048	ΔcrrC	256
ΔsoxS	>2048	ΔkexD	256
ΔnarI	>2048	ΔcrrCkexD	128
ΔentE	>2048	ΔacrAB	256
ΔibpAB	>2048	ΔcrrAB	32
ΔoqxAB	>2048	ΔtolC	16
ΔeptA	2048	ΔphoPQ	8
ΔpmrAB	1024	ΔarnT	<8

Fig. 3. Characterization of the resistance and heteroresistance to PMB of wild-type and deletion mutants of strain E105227 by population analysis profile (PAP) and E-test. Colonies in the inhibition zone of the E-test indicate a heteroresistance phenotype, in which a subpopulation shows higher resistance to PMB than the overall population. (A and B) Deletion mutants in metabolic genes highly upregulated in response to PMB (A) and in genes related to PMB resistance in other bacteria (B), which did not show changes in resistance or heteroresistance in comparison with the parental strain. (C) Deletion mutants with reduced PMB resistance. (D) MIC data for all strains by broth microdilution.

PRED [56] indicates this protein has similarities to D-alanine-D-alanine ligases participating in the assembly of bacterial cell wall precursors [57]. KexD is the membrane component of an RND-type efflux pump protein that was first identified in *K. pneumoniae* as associated to PMB and colistin resistance [24], and more recently in several PMB-resistant *Enterobacter* species [23]. RND-type efflux pumps form a tripartite protein complex involving a periplasmic enzyme and an outer membrane protein channel [58]. Like in *K. pneumoniae*, no other genes encoding additional RND efflux pump components were observed in the vicinity of *kexD*, suggesting that the periplasmic protein AcrA and the outer membrane channel TolC could be utilized in *Enterobacter* as they are in *K. pneumoniae* [59]. Therefore, we also constructed deletion mutants lacking AcrAB and TolC. One additional *acrA* homologue in *E. bugandensis*, identified as *oqxA* (E105227_02269, [34]), was also upregulated in response to PMB ($Log_2FC = 2.7$). OqxAB proteins form an RND-type efflux pump involved in antibiotic resistance [60]. Because OqxA protein could also contribute to KexD function, we constructed a deletion of the *oqxAB* genes. The genes *crrC, kexD*, and 02669 are present in a gene cluster that also contains homologues of the *crrab* genes that encode a two-component regulator. In *K. pneumoniae*, H239_3059, *crrC*, and *kexD* are regulated by CrrAB [24,61,62]; therefore, we also constructed a Δ*crrAB* mutant.

Based on PAP and MIC by broth microdilution and E-test (Fig. 3), the deletion mutants could be assigned to two groups. The first group, including Δ*oqxAB*, Δ*eptA*, Δ*pmrAB*, and Δ*02669*, did not show any differences in PMB resistance and heteroresistance (Fig. 3B), and despite Δ*pmrAB* and Δ*02669* showed reproducibly less colonies in the inhibition area of the E-test, no differences in the PAP were observed when compared with the parental isolate (Fig. 3B). The lack of EptA-mediated PEtN modification was confirmed by the lipid A MALDI TOF MS analysis of Δ*pmrAB* and Δ*eptA*, both in the absence and upon challenge with PMB, which shows the characteristic ion peak of 1955 *m/z* denoting the presence of L-Ara4N in both growth conditions and no peaks associated with the PEtN modification (Fig. 4A). The absence of PEtN could not be explained by a technical issue with MALDI-TOF MF analysis because ion peaks indicating PEtN lipid A modification appeared in a strain of *Enterobacter kobei*, whose lipid A was examined under the same conditions (Supplementary Fig. S4).

The second group of mutants, including Δ*crrC,* Δ*kexD,* Δ*acrAB,* Δ*crrAB,* Δ*tolC,* Δ*phoPQ,* and Δ*arnT*, showed significant differences in the PAP for PMB, indicating that these mutations affected both resistance and heteroresistance. From these, Δ*crrAB*, Δ*tolC,* Δ*phoPQ,* and Δ*arnT* clearly lost the heteroresistance phenotype (Fig. 3C) and they were the most sensitive to PMB (MIC ≤32 μg/mL; Fig. 3D). This suggests that the addition of L-Ara4N to the lipid A, which depends on PhoPQ regulation of the *arn* operon, is critical for PMB resistance in *E. bugandensis*, as shown before in *E. cloacae* [12]. MALDI TOF MS analysis of the lipid A from the Δ*phoPQ* and Δ*arnT* mutants confirmed the loss of the 1955 *m/z* ion peak, and both mutants were unable to survive challenge with 0.1 μg/mL PMB (Fig. 4B). Moreover, our results demonstrate that efflux pumps are critical for PMB resistance, as suggested by the reduced resistance upon deletion of the *tolC* gene, which encodes an outer-membrane channel protein that is essential for the function of multiple drug efflux pumps. The loss of *tolC* function can also affect bacterial fitness; however, we have shown that Δ*tolC* has only a modest reduction in fitness (Supplementary Fig. S5), while displaying a severe reduction in sensitivity to PMB (MIC = 16 ug/mL; Fig. 3D) and loss of heteroresistance (Fig. 3C, Supplementary Fig. S5). Moreover, our data are consistent with the finding that KexD and AcrAB are also required for PMB resistance (Fig. 3C). The double mutant Δ*crrCkexD* had a stronger effect in the reduction of PMB resistance, suggesting that both proteins have a synergistic effect. However, the Δ*crrAB* mutant exhibited a higher reduction in the MIC, suggesting that CrrAB could regulate the expression of other unidentified genes, in addition to *crrC* and *kexD,* also involved in PMB resistance. As expected, lipid A MS analyses in these mutants revealed the presence of the 1955 *m/z* ion peak (Fig. 4C), confirming that their increased susceptibility to PMB does not depend on L-Ara4N modifications.

3.4. Complementation and heterologous expression of crrC and kexD in E. ludwigii and E. coli K-12 indicate a role for these genes in PMB resistance

To validate the previous results, the Δ*crrC*, Δ*kexD*, and Δ*crrCkexD* mutants were genetically complemented with the respective parental genes expressed under the control of the constitutive trimethoprim promoter (Supplementary Table S1). PAP and E-test assays demonstrated that the complemented mutants recovered the wild-type phenotype (Fig. 5A), showing greater levels of resistance to PMB, likely due to gene overexpression, while complementation did not occur in the presence of the empty plasmid (Fig. 5A). We also investigated whether *crrC* and *kexD* can influence PMB resistance in bacteria that normally lack both genes. Therefore, we carried out heterologous reconstitution of PMB resistance in a PMB-sensitive *E. ludwigii* (strain E2618) and in the *E. coli* K12 W3110. The *E. ludwigii* E2618 MIC against PMB was 4–8 μg/mL, while *E. coli* W3110 was sensitive to <2 μg/mL (Fig. 5B). After overexpression of CrrC, KexD, or CrrCKexD in E2618 and W3110, the PAP analysis in E2618 showed increased PMB resistance when the bacteria expressed both genes (Fig. 5B), denoted by an increasing MIC from 8 to >2048 μg/mL. A modest increase was also observed when individually expressing *crrC* or *kexD.* In contrast, overexpression of individual genes in W3110 did not result in differences by E-test with any of the plasmids (Fig. 5B). Increased PMB resistance was noticed according to the PAP results (Fig. 5B), albeit at a much lower level than in E2618. These results suggest that the function of *crrC* and *kexD* could require additional components present in *E. ludwigii* but absent in *E. coli.* The genes E2618_03728 and E2618_03729 in *E. ludwigii* [34], not present in *E. coli* W3110, are orthologues of *E. bugandensis* genes E105227_00743 (encoding a hypothetical lipoprotein) and E105227_00744 (encoding a porin), respectively, and both were found in the top 20 upregulated genes in presence of PMB (Supplementary Table S5). We investigated whether these genes encoded proteins that could play analogous roles as AcrA and TolC by constructing a Δ*03728–29* double deletion mutant in the *E. ludwigii* strain E1618. However, heterologous expression of *crrC* and *kexD* in the Δ*03728–29* mutant did not show any differences in PMB resistance when compared with the parental strain expressing of *crrC* and *kexD*, indicating that E2618_03728 and E2618_03729 are not necessary for the function of KexD (Supplementary Fig. S6).

3.5. Enterobacter virulence in Galleria mellonella does not correlate with PMB resistance

To determine whether PMB resistance correlates with in vivo virulence, we investigated the relative virulence of strains E105227 and E104107 in the *G. mellonella* larvae infection model, following larvae survival daily over five days post-infection. The PMB-sensitive *E. ludwigii* E2618 strain was used as a control. The results indicated that both *E. bugandensis* E105227 and *E. ludwigii* E2618 exhibited low virulence (85% and 92% survival by day 5), while *E. bugandensis* E104107 was significantly more pathogenic (37% larvae survival by day 5; $P < 0.001$) (Supplementary Fig. S7). We concluded that the relative virulence of each isolate was strain dependent and could not be directly correlated with the level of PMB susceptibility, suggesting other factors may also play a role in de-

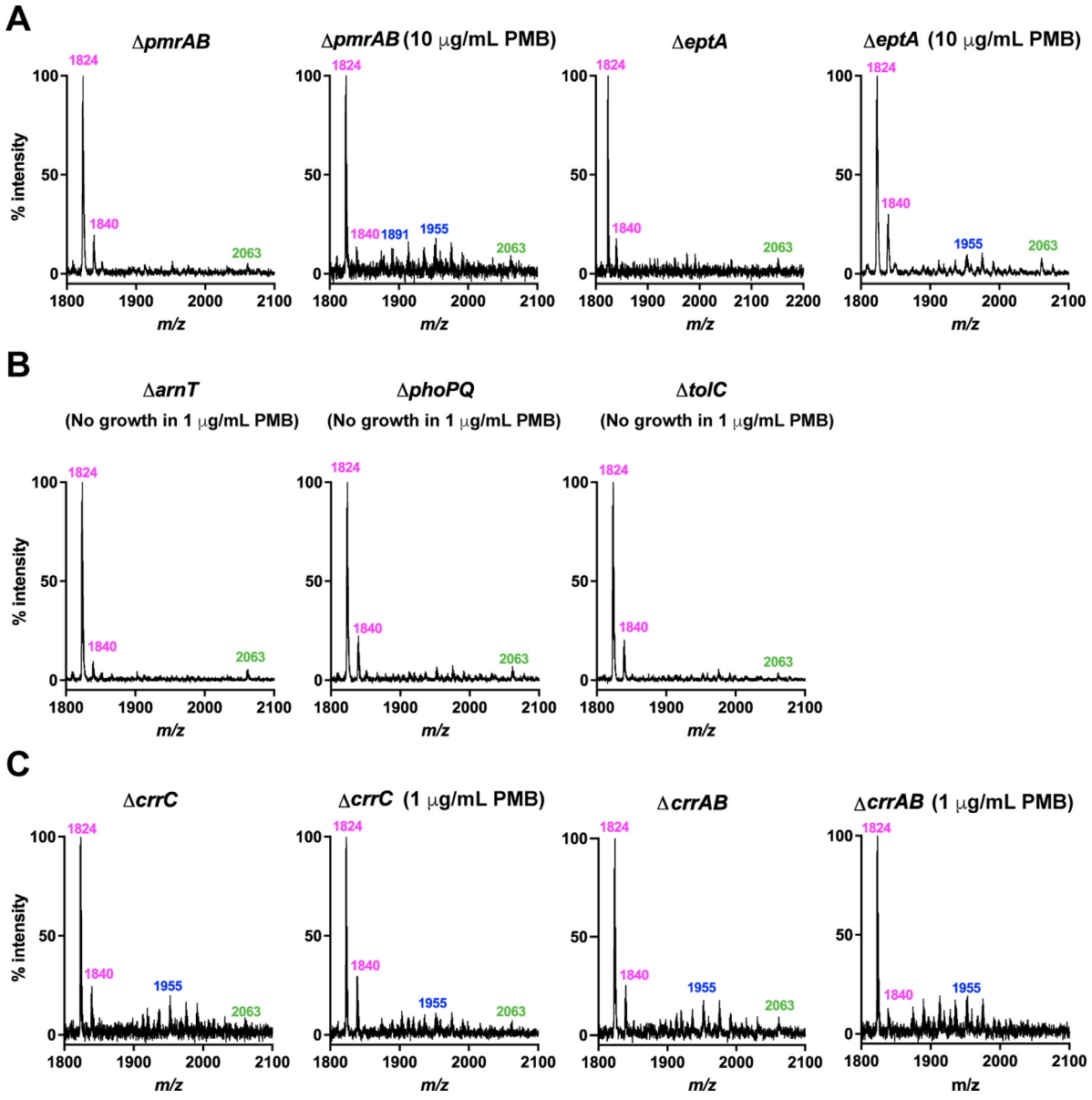

Fig. 4. MALDI-TOF MS profiles of E105227 gene deletion mutants in the presence and absence of PMB challenge. The concentration of PMB varied from 10 μg/mL (panel A) to 1 μg/mL (panel C). Deletion mutants in panel B did not grow at 1 μg/mL PMB and their MS spectra was obtained from medium without PMB.

termining the pathogenicity of *Enterobacter* isolates in the *G. mellonella* model.

3.6. CrrC is a membrane protein that interacts with KexD and AcrB

Based on *in silico* topological analysis, CrrC is a predicted membrane protein comprising four transmembrane helices. Western blot of membrane and soluble cell fractions of Δ*crrC* containing a plasmid expressing CrrC with a C-terminal FLAG fusion ($CrrC_{FLAG}$) confirmed the membrane location of the *E. bugandensis* CrrC, with an apparent molecular mass of 16 kDa (Fig. 6A). As expected, KexDFlag, with an apparent molecular mass of ca. 111 kDa, is also located in the membrane (Fig. 6A). The conserved genetic linkage of the *crrC* and *kexD* genes and the membrane location of the products suggests that both proteins physically interact. We therefore performed pull-downs by separately expressing CrrCFLAG and KexD carrying a C-terminal 6xHis tag (KexD6xHis) and mixing the individual lysates. Western blot analysis after Ni^{2+}-affinity chromatography revealed that KexD6xHis interacted with CrrC, as CrrCFLAG was also identified in the eluted fractions using anti-FLAG antibodies (Fig. 6B). Because KexD and AcrB are structurally similar (see below) and AcrB was also found upregulated in the transcriptomic analysis (Fig. 2), we performed a pull-down experiment with AcrB6xHis, which afforded similar results, indicating that CrrC can also interact with the AcrB pump (Fig. 6B). To confirm these results, we performed co-immunoprecipitations of membrane fractions after chemical crosslinking using CrrCFLAG (in the Δ*crrC* strain) and KexDFLAG (in the Δ*crrC-kexD* strain). Proteins from putative protein complexes that reacted with the anti-FLAG antibody (and comparable regions in the gel from samples carrying empty plasmids) were extracted and subjected to reverse phase liquid chromatography mass spectrometry (LC-MS) for protein identification. The results [34] indicated that CrrC interacted with high-molecular mass complexes above 250 kDa, which contained proteins corresponding to KexD, AcrD, and proteins belonging to the MdtABC efflux pump (Fig. 6C). In the co-IP experiment using KexDFLAG, high molecular weight bands detected by the anti-FLAG antibody contained TolC and AcrA (Fig. 6C), both of

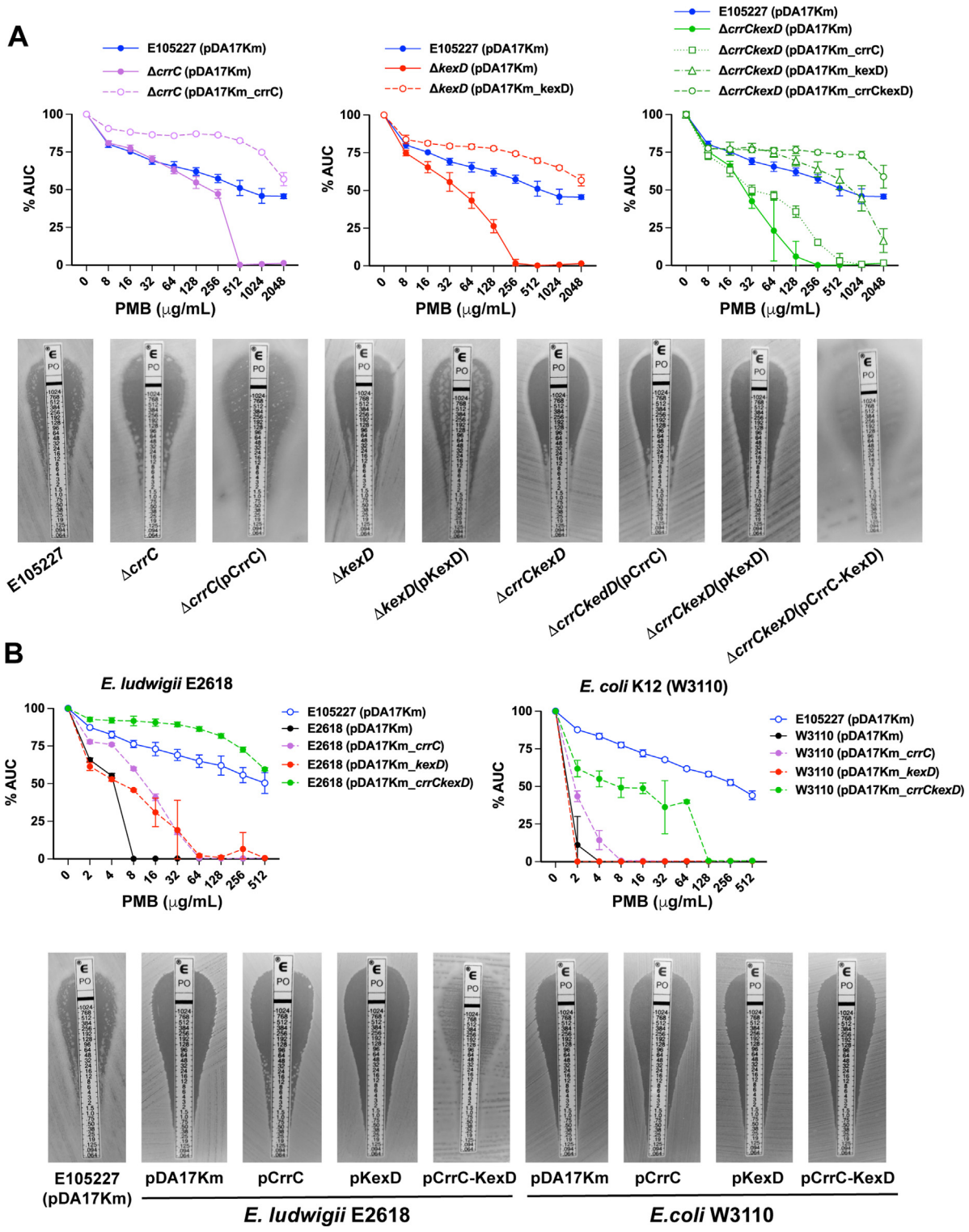

Fig. 5. Genetic complementation experiments. (A) Complementation of E105227 deletion mutants Δ*crrC*, Δ*kexD*, and Δ*crrCkexD*. Continue lines indicate complementation with the empty plasmid, pDA17Km. Dashed lines in the Δ*crrCkexD* graph indicate complementation with *crrC*, *kexD*, or both. The blue lines in all graphs correspond to the PAP of the wild-type strain E105227 with the empty plasmid pDA17Km. The corresponding E-test results for mutants and their complemented versions are shown in the bottom panel. (B) Heterologous complementation of the PMB-sensitive strains *Enterobacter ludwigii* E2618 and *E. coli* K12 (W3110). (C) The corresponding E-test results are shown in the bottom panel.

which were also found upregulated in the transcriptomic analysis and contribute to PMB resistance and heteroresistance (Fig. 3C). Together, the results suggested that CrrC interacts with KexD and AcrB and KexD interacts with TolC and AcrA. KexD does not have an AcrA homolog in the vicinity of the *crrCkexD* operon, in agreement with previous work in *K. pneumoniae* reporting that KexD may use AcrA as the membrane fusion component of the efflux pump, while TolC provides the outer membrane channel [59]. We utilized Alphafold to model KexD and CrrC in a complex (Fig. 7A). The results indicated that both proteins make contacts that involve

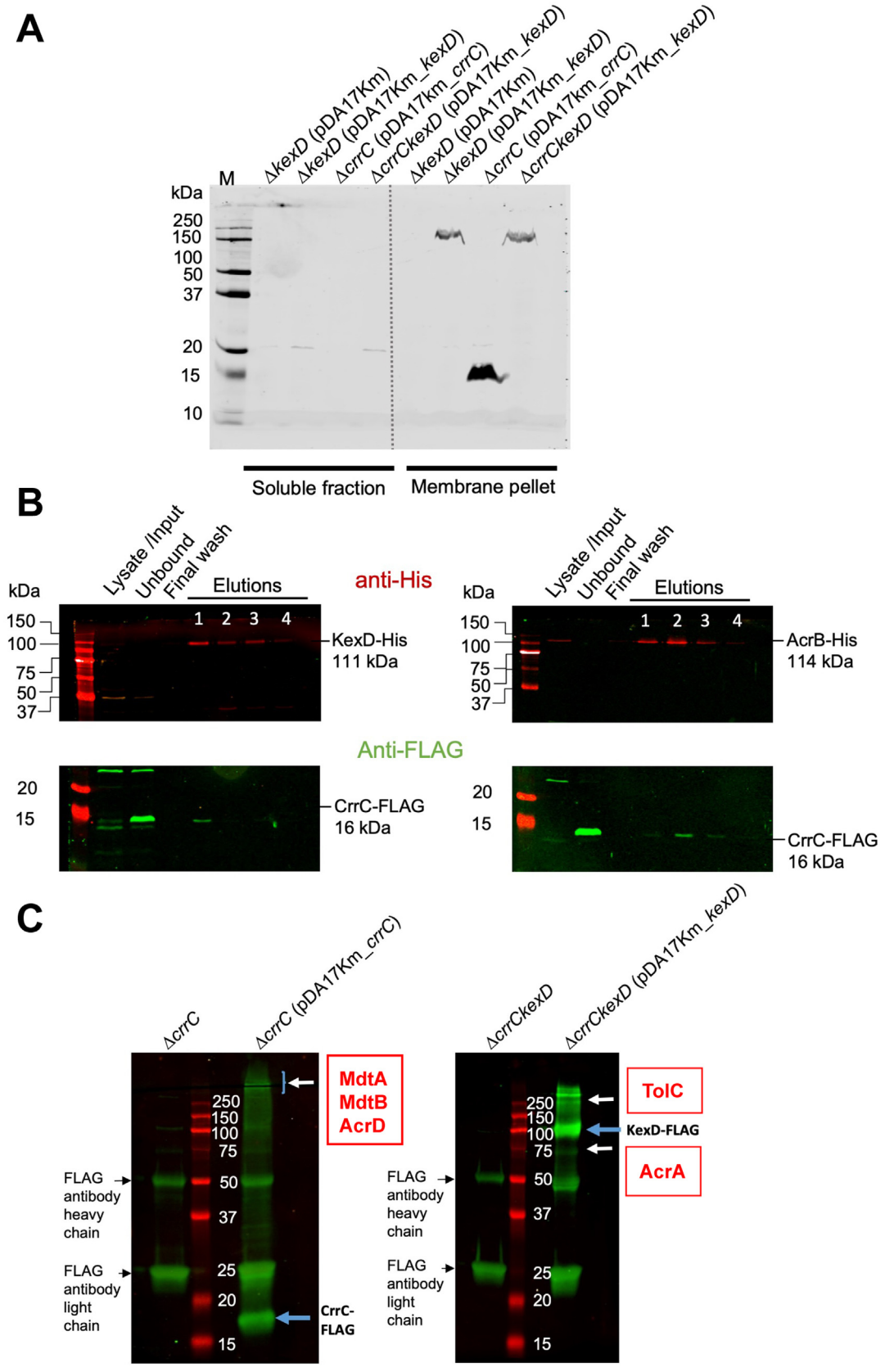

Fig. 6. Characterization of CrrC. (A) Western blot to detect CrrCFLAG and KexDFLAG using anti-FLAG monoclonal antibody in the mutants Δ*crrC* (pIGR02), Δ*kexD* (pIGR05), and Δ*crrCkexD* (pIGR05). Both soluble and membrane fractions were used. (B) Pull-down experiments with CrrCFLAG/KexD6xHis and CrrCFLAG/AcrB6xHis, followed by western bot with anti-FLAG and anti-His antibodies. Lysate/Input, corresponds to a sample before loading the Ni-NTA column; Unbound, corresponds to a sample after the material passes through the Ni-NTA column prior to washed with imidazole. CrrCFLAG and AcrB6xHis are detectable in the lysate, but the expression of KexD6xHis in the lysate is noticeable only after overexposure of the blot, indicating this protein is less expressed, but it becomes detectable after affinity purification. (C) Immunodetection using anti-FLAG antibodies from co-immunoprecipitation assay of CrrCFLA and KexDFLAG. The bands contained by arrows were subjected to proteomic analysis to identify interacting partners. The identity of the proteins in complexes was established by MS and indicated in the red boxes.

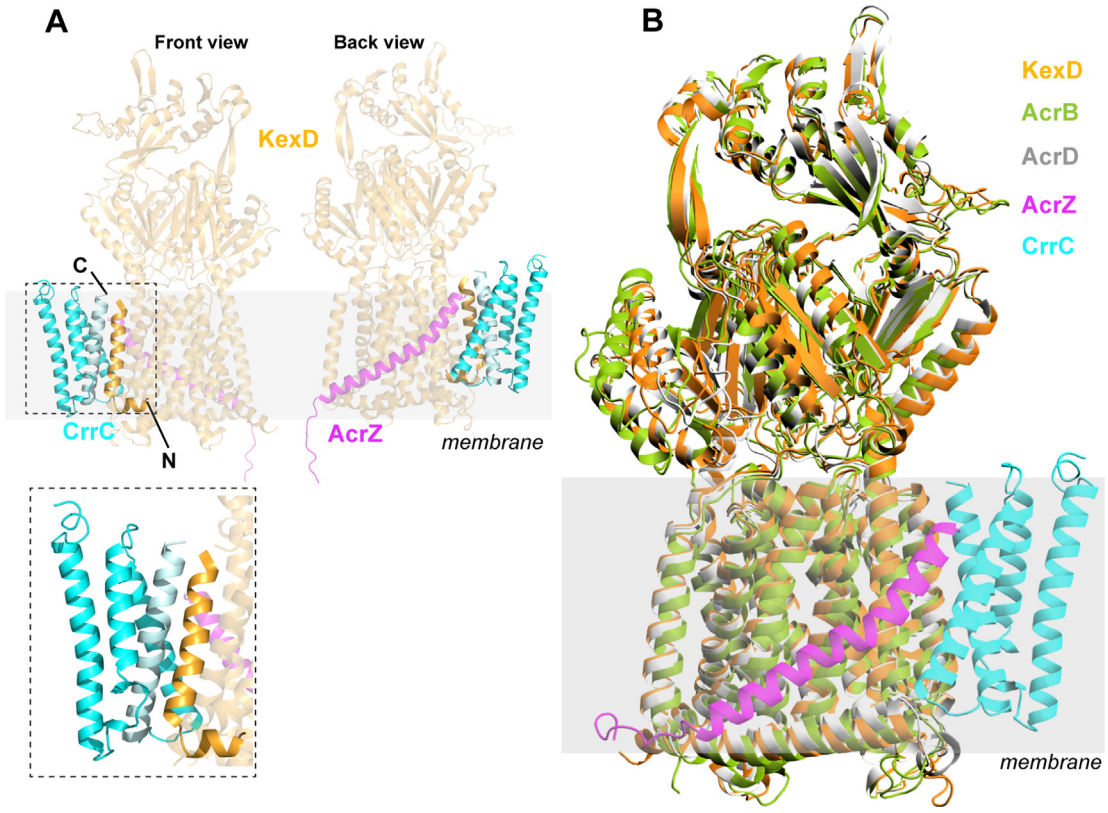

Fig. 7. Structural models of KexD/CrrC complexes were obtained by running Alphafold with Colabfold v1.5.2 (https://colab.research.google.com/github/sokrypton/ColabFold/blob/main/AlphaFold2.ipynb) with default parameters. (A) Alphafold model of KexD (orange) in complex with CrrC (cyan) and AcrZ (PDB 4C48, pink). Front and back views are presented to denote the different regions of KexD interacting with CrrC and AcrZ. The inset provides a more detailed view showing that the C-terminal helix of CrrC interacts with the N-terminal helix of KexD. (B) Structural alignment of KexD (orange), AcrB (PBD 4CDI, green), and AcrD (PDB 8F4R, gray) in complex with CrrC (cyan) and AcrZ (pink).

residues in the N-terminal membrane helix of KexD and residues in the C-terminal helix of CrrC (Fig. 7A). Moreover, the Alphafold KexD structure is almost superimposable to the crystal structures of AcrB and AcrD, demonstrating that the interaction region with CrrC in all these proteins is conserved (Fig. 7B). AcrZ is a small alpha-helical membrane protein that interacts with several transmembrane helices in the membrane domain of the *E. coli* AcrB and plays a role in the regulation of the function of the AcrABTolC efflux pump [21,63,64]. Because an AcrZ homologue is present in *E. bugandensis* we also modelled KexD/AcrZ interactions by Alphafold (Fig. 7A,B), which agreed with the cryoEM structure of the *E. coli* AcrABZTolC complex [64], indicating that the sites of interaction of CrrC and AcrZ with KexD (and AcrB/AcrD membrane domains) are different (Fig. 7B). We did not investigate the association of AcrZ and KexD biochemically because, in contrast, to *crrC, acrZ* is not expressed in response to PMB in both E105227 and in E104107 (normalized log2FoldChange –0.066 and 0.28, respectively [34]), suggesting this protein is not implicated in PMB resistance.

4. Discussion

We demonstrate in this work that the *E. bugandensis* efflux pump membrane subunit KexD and the small transmembrane protein CrrC, whose genes are highly overexpressed in response to PMB, play a significant role in PMB resistance and heteroresistance. Studies in *K. pneumoniae* have suggested that CrrC induces the expression of the *arnBCADTEF* operon and the *pmrC* (*eptA*) gene via the PmrAB TCS [27,61]; however, there is no mechanistic understanding on how this induction occurs. Using biochemical analysis and molecular modelling, we show that CrrC is an integral membrane protein comprising four predicted transmembrane helices. Our results also indicate that PmrAB is not involved in PMB resistance, as shown in previous studies for *Enterobacter* species [12,17], because the *E. bugandensis* Δ*pmrAB* mutant remains resistant to PMB and its lipid A shows the modification with L-Ara4N upon exposure to PMB, suggesting it is unlikely that CrrC in this bacterium could act via PmrAB.

Compared with other RND-like efflux pumps, such as AcrAB or OqxAB, KexD is unusual because it is not encoded in association to a periplasmic anchor, such as AcrA [65]. In *E. coli*, AcrA can function with other RND-like efflux pumps, such as YhiV, AcrD, and AcrF, which are encoded in different regions of the genome from the *acrAB* operon [58]. KexD was suggested to function with AcrA in *K. pneumoniae* [59]. Our co-immunoprecipitation experiments using $KekD_{FLAG}$ as bait, followed by proteomic analysis, suggest that TolC and AcrA interact with KexD; therefore, KexD likely functions with AcrA and TolC, a conclusion supported by the increased PMB susceptibility of the Δ*acrAB* and Δ*tolC* mutants. The observation that Δ*tolC* is more susceptible to PMB than Δ*acrAB* is consistent with the role of TolC as the porin channel for multiple efflux pumps. We biochemically demonstrated by pull down/MS experiments that CrrC interacts not only with KexD but also with AcrB. Alphafold modelling predicts that the C-terminal transmembrane helix of CrrC contacts residues of the N-terminal helix of KexD. Together, our experimental and bioinformatic data suggest that CrrC interacts with KexD and AcrB at the membrane level, possibly regulating the permease function of these pumps. Modelling also revealed that KexD, AcrB, and AcrD are structurally conserved, which explains why these proteins also appear in the CrrC pull-down experiments, indicating they could also interact with CrrC. A prece-

dent for a small membrane protein regulating an efflux pump exists in *E. coli* where AcrZ interacts with the AcrB membrane domain of the AcrABTolC complex [21,63,64]. AcrZ, also present in *E. bugandensis* E105227 and E104107 strains, comprises a single α-helical protein, but there is no conservation between AcrZ and CrrC and the sites of interaction of each protein with the membrane domain of KexD (and AcrB) are also different. The transcription of *acrZ* did not change in response to PMB, indicating this protein is not involved in PMB resistance. In contrast, the high level of *crrC* expression in response to PMB and the requirement of the protein for high-level PMB resistance suggests that CrrC may have evolved to provide a bacterial defence against antimicrobial peptides, either clinically or in polymicrobial communities, such as in the gut.

Apart from Δ*crrAB*, Δ*crrC*, and Δ*kexD*, other mutants, such as Δ*arnT*, Δ*tolC*, Δ*acrAB*, and Δ*phoPQ*, also showed a significant reduction of PMB resistance in *E. bugandensis*, as previously described for the *Enterobacter cloacae* complex [12,18]. The Δ*arnT* was the most sensitive mutant, while Δ*eptA* showed no differences with the wild-type strain in PMB resistance, despite the *eptA* gene was upregulated under PMB exposure. This suggests that the EptA enzyme may be inhibited post-transcriptionally, as recently described [66]. Therefore, we conclude that the Lipid A modification in *E. bugandensis* depends on L-Ara4N addition, but not PEtN. In addition to differential regulation of genes known to be implicated in PMB resistance, our transcriptomic analysis revealed differential expression of many metabolic genes, suggesting that bacteria exposed to PMB are under considerable stress. Despite that individual mutants in some of these genes did not directly affect PMB resistance, it is possible that they reduce the overall fitness of the bacterium under stress driven by the cationic peptides. For example, the only gene involved in siderophore biosynthesis, deleted in this study, was *entE*; however, no decrease of PMB resistance was observed in this mutant. Assuming a deficiency in iron, the impaired enterobactin biosynthesis may be insufficient to disturb the iron acquisition because the bacterium could possess alternative iron uptake systems. Alternatively, production of siderophores could be a response to the oxidative damage caused by PMB [67]. Another enriched category in the RNA-seq data is nitrate assimilation. In our study, the *narI_2* gene encoding the respiratory nitrate reductase 1 gamma chain was deleted, but the deletion had no effect in PMB resistance. E105227 possessed two *narI* copies, but only *narI_2* is upregulated in presence of PMB (*narI_1* is –0.7 Log_2 FC downregulated and *narI_2* is 5.2 Log_2 FC upregulated). In *Pseudomonas aeruginosa*, nitrate respiration could be important under stress by PMB [68], but whether this is the same for *Enterobacter* species remains unknown. We also observed that the level of PMB resistance in *Enterobacter* strains does not correlate with their relative virulence in the *G. mellonella* larvae infection model, indicating that the presence of a PMB-resistant phenotype does not necessarily imply increased pathogenicity.

In conclusion, the PMB resistance in *E. bugandensis* is driven by lipid A modification through the addition of L-Ara4N, which is regulated by PhoPQ and probably other TCS, such as CrrAB, but not by PmrAB. Moreover, resistance is likely potentiated by efflux mediated by AcrAB-TolC and KexD-AcrA-TolC, and possibly other pumps whose activities could be potentiated by CrrC. Together, our data support a two-tier model of resistance to polymyxins: one operating at the outer membrane by reducing the binding of the antimicrobial peptides to the lipopolysaccharide and another one acting in the inner membrane mediated by efflux pumps and possibly membrane lipid modifications.

Funding: The Core Unit SysMed at the University of Würzburg was supported by the IZKF at the University of Würzburg (project Z-6). N.E.S. was supported by an Australian Research Council Future Fellowship (FT200100270) and an ARC Discovery Project Grant (DP210100362). L.M. was supported by a Doctoral Training Program at Queen's University. S.K. was supported by an Internship from the International Association for the Exchange of Students for Technical Experience. This study was supported by grants from the Biotechnology and Biological Sciences Research Council (grant no. BB/T005807/1 and BB/S006281/1) to M.A.V.

Competing interests: The authors have indicated they have no potential conflicts of interest to disclose.

Ethical approval: Not Required

Acknowledgements: We thank Benoît Doublet from Infectiologie Animale et Santé Publique, Nouzilly, 37380, France, for the gift of pKD46-Gm and pCP20-Gm, Shazad Mushtaq, Antimicrobial Resistance and Healthcare Associate Infections Reference Unit, UK Health Security Agency, for the gift of the *Enterobacter* strains used in this research, and the Core Unit SysMed at the University of Würzburg for technical support, RNA-seq data generation and analysis. We also thank the Melbourne Mass Spectrometry and Proteomics Facility of The Bio21 Molecular Science and Biotechnology Institute for access to MS instrumentation.

Supplementary materials

Supplementary material associated with this article can be found, in the online version, at doi:10.1016/j.jgar.2024.03.012.

References

[1] Davin-Regli A, Lavigne JP, Pages JM. *Enterobacter spp.*: Update on taxonomy, clinical aspects, and emerging antimicrobial resistance. Clin Microbiol Rev 2019;32. doi:10.1128/CMR.00002-19.
[2] Zong Z, Feng Y, McNally A. Carbapenem and colistin resistance in *Enterobacter*: Determinants and clones. Trends Microbiol 2021;29:473–6. doi:10.1016/j.tim.2020.12.009.
[3] Binsker U, Kasbohrer A, Hammerl JA. Global colistin use: a review of the emergence of resistant *Enterobacterales* and the impact on their genetic basis. FEMS Microbiol Rev 2022;46. doi:10.1093/femsre/fuab049.
[4] Doijad S, Imirzalioglu C, Yao Y, Pati NB, Falgenhauer L, Hain T, et al. *Enterobacter bugandensis* sp. nov., isolated from neonatal blood. Int J Syst Evol Microbiol 2016;66:968–74. doi:10.1099/ijsem.0.000821.
[5] Hernandez-Alonso E, Bourgeois-Nicolaos N, Lepainteur M, Derouin V, Barreault S, Waalkes A, et al. Contaminated incubators: Source of a multispecies *Enterobacter* outbreak of neonatal sepsis. Microbiol Spectr 2022;10:e0096422. doi:10.1128/spectrum.00964-22.
[6] Girlich D, Ouzani S, Emeraud C, Gauthier L, Bonnin RA, Le Sache N, et al. Uncovering the novel *Enterobacter cloacae* complex species responsible for septic shock deaths in newborns: a cohort study. Lancet Microbe 2021;2:e536–ee44. doi:10.1016/S2666-5247(21)00098-7.
[7] Daugelavicius R, Bakiene E, Bamford DH. Stages of polymyxin B interaction with the *Escherichia coli* cell envelope. Antimicrob Agents Chemother 2000;44:2969–78. doi:10.1128/AAC.44.11.2969-2978.2000.
[8] Sabnis A, Hagart KL, Klockner A, Becce M, Evans LE, Furniss RCD, et al. Colistin kills bacteria by targeting lipopolysaccharide in the cytoplasmic membrane. Elife 2021;10. doi:10.7554/eLife.65836.
[9] Norgan AP, Freese JM, Tuin PM, Cunningham SA, Jeraldo PR, Patel R. Carbapenem- and Colistin-resistant *Enterobacter cloacae* from Delta, Colorado, in 2015. Antimicrob Agents Chemother 2016;60:3141–4. doi:10.1128/AAC.03055-15.
[10] Mushtaq S, Reynolds R, Gilmore MC, Esho O, Adkin R, Garcia-Romero I, et al. Inherent colistin resistance in genogroups of the *Enterobacter cloacae* complex: epidemiological, genetic and biochemical analysis from the BSAC Resistance Surveillance Programme. J Antimicrob Chemother 2020;75:2452–61. doi:10.1093/jac/dkaa201.
[11] Band VI, Crispell EK, Napier BA, Herrera CM, Tharp GK, Vavikolanu K, et al. Antibiotic failure mediated by a resistant subpopulation in *Enterobacter cloacae*. Nat Microbiol 2016;1:16053. doi:10.1038/nmicrobiol.2016.53.
[12] Kang KN, Klein DR, Kazi MI, Guerin F, Cattoir V, Brodbelt JS, Boll JM. Colistin heteroresistance in *Enterobacter cloacae* is regulated by PhoPQ-dependent 4-amino-4-deoxy-L-arabinose addition to lipid A. Mol Microbiol 2019;111:1604–16. doi:10.1111/mmi.14240.

[13] Doijad SP, Gisch N, Frantz R, Kumbhar BV, Falgenhauer J, Imirzalioglu C, et al. Resolving colistin resistance and heteroresistance in *Enterobacter* species. Nat Commun 2023;14:140. doi:10.1038/s41467-022-35717-0.
[14] Band VI, Satola SW, Burd EM, Farley MM, Jacob JT, Weiss DS. Carbapenem-resistant *Klebsiella pneumoniae* exhibiting clinically undetected colistin heteroresistance leads to treatment failure in a murine model of infection. mBio 2018;9. doi:10.1128/mBio.02448-17.
[15] Needham BD, Trent MS. Fortifying the barrier: the impact of lipid A remodelling on bacterial pathogenesis. Nat Rev Microbiol 2013;11:467–81. doi:10.1038/nrmicro3047.
[16] Boll JM, Tucker AT, Klein DR, Beltran AM, Brodbelt JS, Davies BW, Trent MS. Reinforcing lipid A acylation on the cell surface of *Acinetobacter baumannii* promotes cationic antimicrobial peptide resistance and desiccation survival. mBio 2015;6:e00478-15. doi:10.1128/mBio.00478-15.
[17] Guérin F, Isnard C, Sinel C, Morand P, Dhalluin A, Cattoir V, Giard JC. Cluster-dependent colistin hetero-resistance in *Enterobacter cloacae* complex. J Antimicrob Chemother 2016;71:3058–61. doi:10.1093/jac/dkw260.
[18] Huang L, Feng Y, Zong Z. Heterogeneous resistance to colistin in *Enterobacter cloacae* complex due to a new small transmembrane protein. J Antimicrob Chemother 2019;74:2551–8. doi:10.1093/jac/dkz236.
[19] Mhaya A, Bégu D, Tounsi S, Arpin C. MgrB inactivation is responsible for acquired resistance to colistin in *Enterobacter hormaechei* subsp. *steigerwaltii*. Antimicrob Agents Chemother 2020;64. doi:10.1128/AAC.00128-20.
[20] Nang SC, Li J, Velkov T. The rise and spread of *mcr* plasmid-mediated polymyxin resistance. Crit Rev Microbiol 2019;45:131–61. doi:10.1080/1040841X.2018.1492902.
[21] Du D, Wang Z, James NR, Voss JE, Klimont E, Ohene-Agyei T, et al. Structure of the AcrAB-TolC multidrug efflux pump. Nature 2014;509:512–15. doi:10.1038/nature13205.
[22] Telke AA, Olaitan AO, Morand S, Rolain JM. *soxRS* induces colistin heteroresistance in *Enterobacter asburiae* and *Enterobacter cloacae* by regulating the acrAB-tolC efflux pump. J Antimicrob Chemother 2017;72:2715–21. doi:10.1093/jac/dkx215.
[23] Pantel L, Guérin F, Serri M, Gravey F, Houard J, Maurent K, et al. Exploring cluster-dependent antibacterial activities and resistance pathways of NOSO-502 and colistin against *Enterobacter cloacae* complex species. Antimicrob Agents Chemother 2022:e0077622. doi:10.1128/aac.00776-22.
[24] Cheng YH, Lin TL, Lin YT, Wang JT. A putative RND-type efflux pump, H239_3064, contributes to colistin resistance through CrrB in *Klebsiella pneumoniae*. J Antimicrob Chemother 2018;73:1509–16. doi:10.1093/jac/dky054.
[25] Sun L, Rasmussen PK, Bai Y, Chen X, Cai T, Wang J, et al. Proteomic changes of *Klebsiella pneumoniae* in response to colistin treatment and *crrB* mutation-mediated colistin resistance. Antimicrob Agents Chemother 2020;64. doi:10.1128/AAC.02200-19.
[26] Pantel L, Juarez P, Serri M, Boucinha L, Lessoud E, Lanois A, et al. Missense mutations in the CrrB protein mediate odilorhabdin derivative resistance in *Klebsiella pneumoniae*. Antimicrob Agents Chemother 2021:65. doi:10.1128/AAC.00139-21.
[27] Cheng YH, Lin TL, Lin YT, Wang JT. Amino acid substitutions of CrrB responsible for resistance to colistin through CrrC in *Klebsiella pneumoniae*. Antimicrob Agents Chemother 2016;60:3709–16. doi:10.1128/AAC.00009-16.
[28] Datsenko KA, Wanner BL. One-step inactivation of chromosomal genes in *Escherichia coli* K-12 using PCR products. Proc Natl Acad Sci USA 2000;97:6640–5.
[29] Jain C, Rodriguez RL, Phillippy AM, Konstantinidis KT, Aluru S. High throughput ANI analysis of 90K prokaryotic genomes reveals clear species boundaries. Nat Commun 2018;9:5114. doi:10.1038/s41467-018-07641-9.
[30] Meier-Kolthoff JP, Goker M. TYGS is an automated high-throughput platform for state-of-the-art genome-based taxonomy. Nat Commun 2019;10:2182. doi:10.1038/s41467-019-10210-3.
[31] Martin M. Cutadapt removes adapter sequences from high-throughput sequencing reads. EMBnet J 2011;17(1):10. doi:10.14806/ej.17.1.200.
[32] Förstner KU, Vogel J, Sharma CM. READemption-a tool for the computational analysis of deep-sequencing-based transcriptome data. Bioinformatics 2014;30:3421–3. doi:10.1093/bioinformatics/btu533.
[33] Hoffmann S, Otto C, Kurtz S, Sharma CM, Khaitovich P, Vogel J, et al. Fast mapping of short sequences with mismatches, insertions and deletions using index structures. PLoS Comput Biol 2009;5:e1000502. doi:10.1371/journal.pcbi.1000502.
[34] Valvano M, Garcia-Romero I, Srivastava M, Scott N. Mechanisms of polymyxin B resistance and heteroresistance in the sepsis pathogen Enterobacter bugandensis. Mendeley Data 2023. doi:10.17632/tpbv7bnh6n.1.
[35] Love MI, Huber W, Anders S. Moderated estimation of fold change and dispersion for RNA-seq data with DESeq2. Genome Biol 2014;15:550. doi:10.1186/s13059-014-0550-8.
[36] Hernández-Salmerón JE, Moreno-Hagelsieb G. Progress in quickly finding orthologs as reciprocal best hits: comparing blast, last, diamond and MMseqs2. BMC Genomics 2020;21:741. doi:10.1186/s12864-020-07132-6.
[37] Oliveros JC. Venny. An interactive tool for comparing lists with Venn's diagrams. https://bioinfogp.cnb.csic.es/tools/venny/index.html. 2007-2015.
[38] Alexa A, Rahnenfuhrer J, Lengauer T. Improved scoring of functional groups from gene expression data by decorrelating GO graph structure. Bioinformatics 2006;22:1600–7. doi:10.1093/bioinformatics/btl140.
[39] Mangas EL, Rubio A, Alvarez-Marin R, Labrador-Herrera G, Pachon J, Pachon-Ibanez ME, et al. Pangenome of *Acinetobacter baumannii* uncovers two groups of genomes, one of them with genes involved in CRISPR/Cas defence systems associated with the absence of plasmids and exclusive genes for biofilm formation. Microb Genom 2019;5. doi:10.1099/mgen.0.000309.
[40] Matthews LR, Vaglio P, Reboul J, Ge H, Davis BP, Garrels J, et al. Identification of potential interaction networks using sequence-based searches for conserved protein-protein interactions or "interologs". Genome Res 2001;11:2120–6. doi:10.1101/gr.205301.
[41] Sonnhammer EL, InParanoid Östlund G. 8: orthology analysis between 273 proteomes, mostly eukaryotic. Nucleic Acids Res 2015;43:D234–9. doi:10.1093/nar/gku1203.
[42] Shannon P, Markiel A, Ozier O, Baliga NS, Wang JT, Ramage D, et al. Cytoscape: a software environment for integrated models of biomolecular interaction networks. Genome Res 2003;13:2498–504. doi:10.1101/gr.1239303.
[43] El-Halfawy OM, Valvano MA. Chemical communication of antibiotic resistance by a highly resistant subpopulation of bacterial cells. PLoS One 2013;8:e68874. doi:10.1371/journal.pone.0068874.
[44] El-Halfawy OM, Valvano MA. Antimicrobial heteroresistance: an emerging field in need of clarity. Clin Microbiol Rev 2015;28:191–207. doi:10.1128/CMR.00058-14.
[45] Gibson DG, Young L, Chuan R-Y, Venter JC, Hutchinson CA, Smith HO. Enzymatic assembly of DNA molecules up to several hundred kilobases. Nature Methods 2009;6:343–5.
[46] Shevchenko A, Tomas H, Havlis J, Olsen JV, Mann M. In-gel digestion for mass spectrometric characterization of proteins and proteomes. Nat Protoc 2006;1:2856–60. doi:10.1038/nprot.2006.468.
[47] Cox J, Mann M. MaxQuant enables high peptide identification rates, individualized p.p.b.-range mass accuracies and proteome-wide protein quantification. Nat Biotechnol 2008;26:1367–72. doi:10.1038/nbt.1511.
[48] Tyanova S, Temu T, Sinitcyn P, Carlson A, Hein MY, Geiger T, et al. The Perseus computational platform for comprehensive analysis of (prote)omics data. Nat Methods 2016;13:731–40. doi:10.1038/nmeth.3901.
[49] Kocsis B, Kilar A, Peter S, Dornyei A, Sandor V, Kilar F. Mass spectrometry for profiling LOS and lipid A structures from whole-cell lysates: Directly from a few bacterial colonies or from liquid broth cultures. Methods Mol Biol 2017;1600:187–98. doi:10.1007/978-1-4939-6958-6_17.
[50] Simar S, Sibley D, Ashcraft D, Pankey G. Colistin and polymyxin B minimal inhibitory concentrations determined by Etest found unreliable for Gram-negative bacilli. Ochsner J 2017;17:239–42.
[51] Torres DA, HMB Seth-Smith, Joosse N, Lang C, Dubuis O, Nuesch-Inderbinen M, et al. Colistin resistance in Gram-negative bacteria analysed by five phenotypic assays and inference of the underlying genomic mechanisms. BMC Microbiol 2021;21:321. doi:10.1186/s12866-021-02388-8.
[52] Kulengowski B, Ribes JA, Burgess DS. Polymyxin B Etest® compared with gold-standard broth microdilution in carbapenem-resistant Enterobacteriaceae exhibiting a wide range of polymyxin B MICs. Clin Microbiol Infect 2019;25:92–5. doi:10.1016/j.cmi.2018.04.008.
[53] Parra-Lopez C, Lin R, Aspedon A, Groisman EA. A *Salmonella* protein that is required for resistance to antimicrobial peptides and transport of potassium. Embo J 1994;13:3964–72.
[54] Giacomucci S, Cros CD, Perron X, Mathieu-Denoncourt A, Duperthuy M. Flagella-dependent inhibition of biofilm formation by sub-inhibitory concentration of polymyxin B in *Vibrio cholerae*. PLoS One 2019;14:e0221431. doi:10.1371/journal.pone.0221431.
[55] Loutet SA, Di Lorenzo F, Clarke C, Molinaro A, Valvano MA. Transcriptional responses of *Burkholderia cenocepacia* to polymyxin B in isogenic strains with diverse polymyxin B resistance phenotypes. BMC Genomics 2011;12:472.
[56] Gabler F, Nam SZ, Till S, Mirdita M, Steinegger M, Soding J, et al. Protein Sequence Analysis Using the MPI Bioinformatics Toolkit. Curr Protoc Bioinformatics 2020;72:e108. doi:10.1002/cpbi.108.
[57] Wu D, Zhang L, Kong Y, Du J, Chen S, Chen J, et al. Enzymatic characterization and crystal structure analysis of the D-alanine-D-alanine ligase from *Helicobacter pylori*. Proteins 2008;72:1148–60. doi:10.1002/prot.22009.
[58] Alav I, Kobylka J, Kuth MS, Pos KM, Picard M, Blair JMA, Bavro VN. Structure, assembly, and function of tripartite efflux and type 1 secretion systems in Gram-negative bacteria. Chem Rev 2021;121:5479–596. doi:10.1021/acs.chemrev.1c00055.
[59] Ogawa W, Onishi M, Ni R, Tsuchiya T, Kuroda T. Functional study of the novel multidrug efflux pump KexD from *Klebsiella pneumoniae*. Gene 2012;498:177–82. doi:10.1016/j.gene.2012.02.008.
[60] Hansen LH, Johannesen E, Burmølle M, Sørensen AH, Sørensen SJ. Plasmid-encoded multidrug efflux pump conferring resistance to olaquindox in *Escherichia coli*. Antimicrob Agents Chemother 2004;48:3332–7. doi:10.1128/AAC.48.9.3332-3337.2004.
[61] Wright MS, Suzuki Y, Jones MB, Marshall SH, Rudin SD, van Duin D, et al. Genomic and transcriptomic analyses of colistin-resistant clinical isolates of *Klebsiella pneumoniae* reveal multiple pathways of resistance. Antimicrob Agents Chemother 2015;59:536–43. doi:10.1128/AAC.04037-14.
[62] McConville TH, Annavajhala MK, Giddins MJ, Macesic N, Herrera CM, Rozenberg FD, et al. CrrB positively regulates high-level polymyxin resistance and virulence in *Klebsiella pneumoniae*. Cell Rep 2020;33:108313. doi:10.1016/j.celrep.2020.108313.
[63] Hobbs EC, Yin X, Paul BJ, Astarita JL, Storz G. Conserved small protein associates with the multidrug efflux pump AcrB and differentially affects antibiotic resistance. Proc Natl Acad Sci U S A 2012;109:16696–701. doi:10.1073/pnas.1210093109.

[64] Wang Z, Fan G, Hryc CF, Blaza JN, Serysheva II, Schmid MF, et al. An allosteric transport mechanism for the AcrAB-TolC multidrug efflux pump. Elife 2017;6. doi:10.7554/eLife.24905.
[65] Ni RT, Onishi M, Mizusawa M, Kitagawa R, Kishino T, Matsubara F, et al. The role of RND-type efflux pumps in multidrug-resistant mutants of *Klebsiella pneumoniae*. Sci Rep 2020;10:10876. doi:10.1038/s41598-020-67820-x.
[66] Purcell AB, Voss BJ, Trent MS. Diacylglycerol kinase A is essential for polymyxin resistance provided by EptA, MCR-1, and other lipid A phosphoethanolamine transferases. J Bacteriol 2022;204:e0049821. doi:10.1128/JB.00498-21.
[67] Yu Z, Zhu Y, Qin W, Yin J, Qiu J. Oxidative stress induced by polymyxin E is involved in rapid killing of *Paenibacillus polymyxa*. Biomed Res Int 2017;2017:5437139. doi:10.1155/2017/5437139.
[68] Kim BO, Jang HJ, Chung IY, Bae HW, Kim ES, Cho YH. Nitrate respiration promotes polymyxin B resistance in *Pseudomonas aeruginosa*. Antioxid Redox Signal 2021;34:442–51. doi:10.1089/ars.2019.7924.